Llywodraeth Cymru
Welsh Government

Yr Is-adran Gwyddoniaeth, Ymchwil a Thystiolaeth
Science, Research, Evidence Division
Y Grŵp Iechyd, Gofal ac Atal
Health, Care and Prevention Group

Influenza compartment transmission model methodology report

21 September 2026

gov.wales

Table of Contents

Introduction

Influenza is an acute viral respiratory infection caused by three virus types: A, B, and C[1]. Most illnesses are due to influenza A and B. Influenza A is responsible for annual seasonal outbreaks and occasionally large epidemics, while influenza B generally causes smaller outbreaks, with the greatest burden in children, where severity can be similar to influenza A.

Seasonal influenza is a major contributor to respiratory morbidity and places significant pressure on healthcare services in Wales each winter. During the winters of 2020/21 and 2021/22, influenza activity and associated hospital admissions remained unusually low, largely due to the implementation of social distancing measures and changes in social mixing patterns due to the COVID-19 pandemic. However, influenza activity resurged from the 2022/23 season onwards as these measures were removed and population mixing returned to more typical levels.

In the 2022/23 season, weekly general practitioner (GP) consultations for influenza-like illness (ILI) in Wales exceeded the baseline Moving Epidemic Method (MEM) threshold of 10.97 per 100,000 population between week 49 of 2022 and week 2 of 2023 [2]. During this season, the dominant circulating influenza subtypes were A(H1N1) and A(H3N2), with a total of 3,892 influenza-related hospital admissions were recorded between September and March [3],[4], [5]. In the 2023/24 and 2024/25 seasons, influenza A(H1N1) was the predominant circulating subtype in Wales, and a total of 2,437 and 4,349 hospital admissions were recorded over the same period [6].

---

[1] **Influenza: the green book, chapter 19**

[2] **Moving Epidemic Method (MEM) is a method used to establish epidemic thresholds for influenza and other respiratory viruses by analysing historical surveillance data to identify pre-epidemic, epidemic, and post-epidemic periods.**

[3] **Science Research Evidence: winter modelling 2025 to 2026**

[4] **Influenza Season in Wales: 2022/23**

[5] **Hospital admissions are calculated using the PEDW dataset using the ICD-10 codes: J09-J11**

[6] **Influenza Season in Wales: 2023/24**

The aim of this paper is to construct a compartmental transmission model to generate projections of medium-term influenza hospital admissions in Wales. This model will be calibrated using historical admissions data from previous seasons and will be used to simulate various scenarios that incorporate different assumptions about vaccine uptake. These scenarios will be used as a part of the winter modelling report 2026-27. It should be noted that the model medium-term projections give a range of outbreak trajectories under different scenarios based on previous season, as opposed to offering a specific, unconditional estimate of what “will” happen.

This paper is currently undergoing peer review. Feedback has been sought from experts, and the model will be put through this year’s Welsh Government modelling annual review assurance framework process. For transparency, we wanted to share the methodology underlying the winter modelling work carried out by SRE, but caution should be taken whilst using the outputs of this paper as the model is currently under review.

Methods

Data Sources

Population data

Population data for Wales were obtained from the Office for National Statistics (ONS) 2023,2024 and 2025 mid-year population estimates [7]. The population was grouped into the following age bands: 0–5 years, 6–17 years, 18–44 years, 45–64 years, and 65 years and over. The population was not stratified by risk status, were chosen to align with available admissions, vaccination, and contact data and to capture key differences in influenza transmission and disease severity across the population.

Contact matrix data

Age-specific contact rates were obtained from the ReCoNNECT social contact survey, which measured social mixing patterns in the United Kingdom following the COVID-19 pandemic. These contact patterns were used to represent non-random mixing between age groups within the transmission model [8] The original contact rates were aggregated to match the five population age groups used in the model using the *socialmatrix* package.[9] The resulting matrix describes the average number of daily contacts between individuals in different age groups and forms the basis of the force of infection within the model.

Influenza subtype data

Influenza subtype data based on samples submitted for virological testing was obtained from Public Health Wales.[10] Here, the data was classified into 4 groups: Influenza A(H1N1), influenza A(H3N2), influenza B and untyped influenza A. Subtype data was not stratified by age.

---

[7] **Population estimates for England and Wales**

[8] **Social contact patterns in the United Kingdom following the COVID-19 pandemic: The Reconnect cross-sectional survey | PLOS Medicine**

[9] **socialmixr: Social Mixing Matrices for Infectious Disease Modelling**

[10] **Weekly Influenza and Acute Respiratory Infection Report - Public Health Wales**

Hospital admissions data

Influenza-related hospital admissions data were obtained from Digital Health Care for Wales (DHCW). Influenza admissions were identified using the following

ICD-10 codes:

- J09X – Influenza due to identified novel influenza A virus
- J100 – Influenza due to other identified influenza virus with pneumonia
- J101 – Influenza due to other identified influenza virus with other respiratory manifestations
- J102 – Influenza due to other identified influenza virus with gastrointestinal manifestations
- J108 – Influenza due to other identified influenza virus with other manifestations
- J110 – Influenza due to unidentified influenza virus with pneumonia
- J111 – Influenza due to unidentified influenza virus with other respiratory manifestations
- J112 – Influenza due to unidentified influenza virus with gastrointestinal manifestations
- J118 – Influenza due to unidentified influenza virus with other manifestations

As not all flu admissions were subtyped, admissions were grouped into five age categories mentioned above and then combined with subtype data.

School holidays data

School holiday calendars were obtained from official school term dates published by the Welsh Government.[11]These data were used to account for changes in social mixing during holiday periods, particularly among school-aged children. Within the transmission model, age-specific contact rates involving school-aged populations were reduced during school holiday periods using a scalar parameter, $h_{\{i,j\}}$. This adjustment reflects

[11] **approved-school-term-dates-2022-to-2023.pdf**

the reduction in school-based contacts and the associated decrease in transmission opportunities during holiday periods. (Please see Annex for more details).

Model structure

Figure 1: Compartment transmission model for modelling influenza admissions

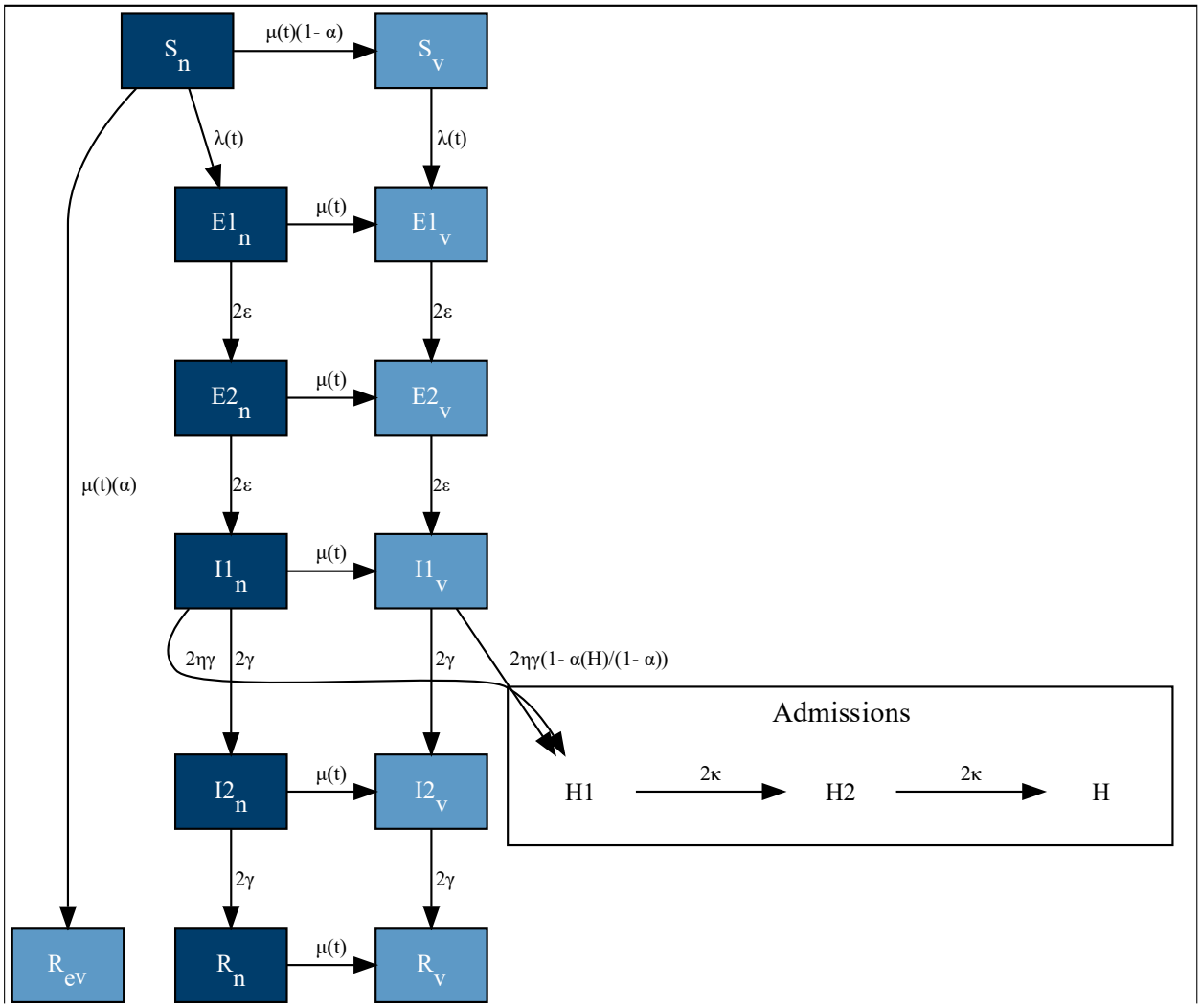

An age-stratified deterministic compartmental transmission model with a fixed population size and non-random age-specific mixing was used to simulate transmission and associated hospital admissions in Wales. The model structure was based on a modified SEIR framework and is designed to capture both infection dynamics and vaccination effects across heterogeneous age groups. Within each age group, individuals were assigned to epidemiological compartments describing disease state and vaccination status. The model comprised susceptible (S), exposed, infectious (I), and recovered (R) compartments, with an Erlang-type staging structure used for both the exposed and infectious periods. Specifically, both the latent and infectious stages

are divided into two sequential compartments ($E1$, $E2$ and $I1$, $I2$ respectively). This formulation generates gamma-distributed waiting times, reducing the variance associated with exponentially distributed residence times and providing a more realistic representation of disease progression.

Individuals progress from the susceptible compartment (S), to the exposed compartments ($E1, E2$) through infection at the force of infection, λ. Following the latent period, individuals move through the exposed compartments at rate ϵ (loss of latency). Individuals then enter infectious compartments ($11, I2$) and recover at rate γ (loss of infectiousness). Following recovery, individuals move to the recovered compartment (R) and are assumed to be immune for the remainder of the simulated season.

Vaccination is represented through parallel compartmental structure. For each epidemiological state, individuals may be either unvaccinated (subscript n) or vaccinated (subscript v). Vaccinated individuals are further partitioned into [12]:

- Effectively vaccinated individuals, who are assumed to have protection against infection and move into a protected recovered state (R_{ev}), and
- Ineffectively vaccinated individuals, who follow the same infection pathway as unvaccinated individuals but remain within vaccinated compartments.

Vaccination reduces susceptibility to infection and, conditional on infection, reduces the probability of hospitalisation. Vaccine effectiveness against infection is denoted by α, while protection against hospitalisation is denoted by $\alpha(H)$. Vaccine protection is assumed to act immediately upon administration and to remain constant over the modelled period.

Vaccination is restricted to individuals aged 65 years and above and those aged 6-64 years classified as at risk, with vaccination occurring at a time-varying rate, $\mu(t)$, reflecting the seasonal vaccination programme.

[12] **Goodfellow et al. 2025**

Hospital admissions are modelled as a probabilistic outcome of infectious individuals. A proportion of individuals in the first infectious stage ($I1_n$ and $I1_v$) progress to hospitalisation at rate η, where η represents the proportion of infectious cases that are hospitalised. To represent the delay between infection and admission, a two-stage Erlang structure ($H1$, $H2$) is used, producing gamma-distributed waiting times[13], the parameter governs the rate of progression through these states and therefore represents the time delay from being infectious to getting hospitalised. Admissions are aggregated across age groups to generate the model output used for calibration against observed weekly influenza admissions.

The differential equations for the model are described in the Annex.

Force of infection

The force of infection for age group i is given by the equation:

$$\lambda_i(t) \quad = (b_0 + b_1 exp(t-\phi)^2/\psi^2) \sum_{i=1} \sigma_i c_{ij}\, h_{ij}\left[I1_{n,j} + I2_{n,j} + I1_{v,j} + I2_{v,j}\right]$$

The force of infection (λ) was modelled as a time-varying exponential function, where parameter b_0 represents the baseline transmission rate, while b_1 scales the seasonal increase in transmission. Parameters ϕ and ψ dictate the timing and width of the epidemic curve. σ_i represents susceptibility, c_{ij} represents the age-specific contact rate and h_{ij} is a scaling parameter that represents the reduction in contact rate during school holidays.

The model assumes a closed population, fixed age-specific contact patterns, no waning immunity within a season, and independent transmission dynamics for each influenza subtype. A full list of assumptions is provided in the Annex.

[13] **Influenza hospital admissions prevented by vaccination: a transmission dynamic analysis of the 2022/2023 and 2023/2024 programmes in England**

Model outputs: The primary model output was the number of new influenza hospital admissions over time. Hospital admissions were generated from transitions through the hospitalisation compartments and aggregated by age group and week to enable comparison with observed influenza admissions data. These weekly admissions were used as the calibration target during parameter inference and subsequently formed the basis of scenario projections.

MCMC based parameter inference

MCMC runs parameters

The transmission model was calibrated to weekly influenza admissions data using Bayesian inference framework. Several key epidemiological parameters, therefore, Markov chain Monte Carlo (MCMC) methods were used to infer their posterior distributions while accounting for uncertainty in both the model and observed data.

Parameter estimation was performed separately for each influenza subtype (A(H1N1), A(H3N2), and B) and for each winter season (2022/23 and 2023/24), resulting in six independent model fits. Separate fitting was undertaken because circulating influenza strains, population immunity, and vaccine effectiveness varied between seasons and subtypes.

Three Markov chains were run for 10,000 iterations, with the first 5,000 iterations discarded as burn-in and the remaining 5,000 iterations used as the empirical samples for the posterior distributions for each of the parameters. As some of the parameters showed correlations, parallel tempering with 10 rungs was used to improve mixing and exploration of the parameter space.

To generate posterior samples, three chains were randomly sampled 100 times (No thinning was performed). Further details of the likelihood calculation and prior distributions are described in the Annex.

MCMC diagnostic

Model convergence was assessed using trace plots and Gelman Rubin diagnostics, with values below 1.1 considered acceptable Effective sample sizes (ESS) were also

calculated for all inferred parameters, with a minimum threshold of 100 used to assess adequate sampling.

Posterior predictive checks and scoring metrics

Model performance was evaluated using weighted interval scores, bias, and interval coverage. In addition, peak height and peak timing of influenza admissions were compared between model outputs and observed data to assess the model's ability to capture the temporal dynamics of Influenza transmission.

Projections for the winter of 2026/27

Admissions projections were created using the calibrated transmission model to explore how different levels of vaccine uptake could influence influenza hospital admissions across multiple subtypes and seasons. For each scenario, the model was re-run using posterior parameter samples from the MCMC inference, while varying vaccine uptake and holding vaccine effectiveness constant. The process was repeated for all subtypes across the three winters. The admissions were then summed across all subtypes to provide total burden estimates giving rise to 12 scenarios in total (4 vaccine uptake assumptions, 3 winters). These projections reflect plausible pre-season trajectories based on historical data and model assumptions and will not be re-calibrated to emerging data during the 2026/27 winter.

Table 1: Scenarios and their underlying assumptions

Assumption	Description of vaccine uptake
No coverage	0%
Low coverage	20% lower than observed coverage
Baseline coverage	Observed vaccine coverage
High coverage	20% higher than observed coverage

Results

Model calibration and posterior distributions

Figure 2: Comparison of model fit and observed weekly influenza admissions during the winter of 2022/23, 2023/24 and 2024/25, in Wales, by subtype

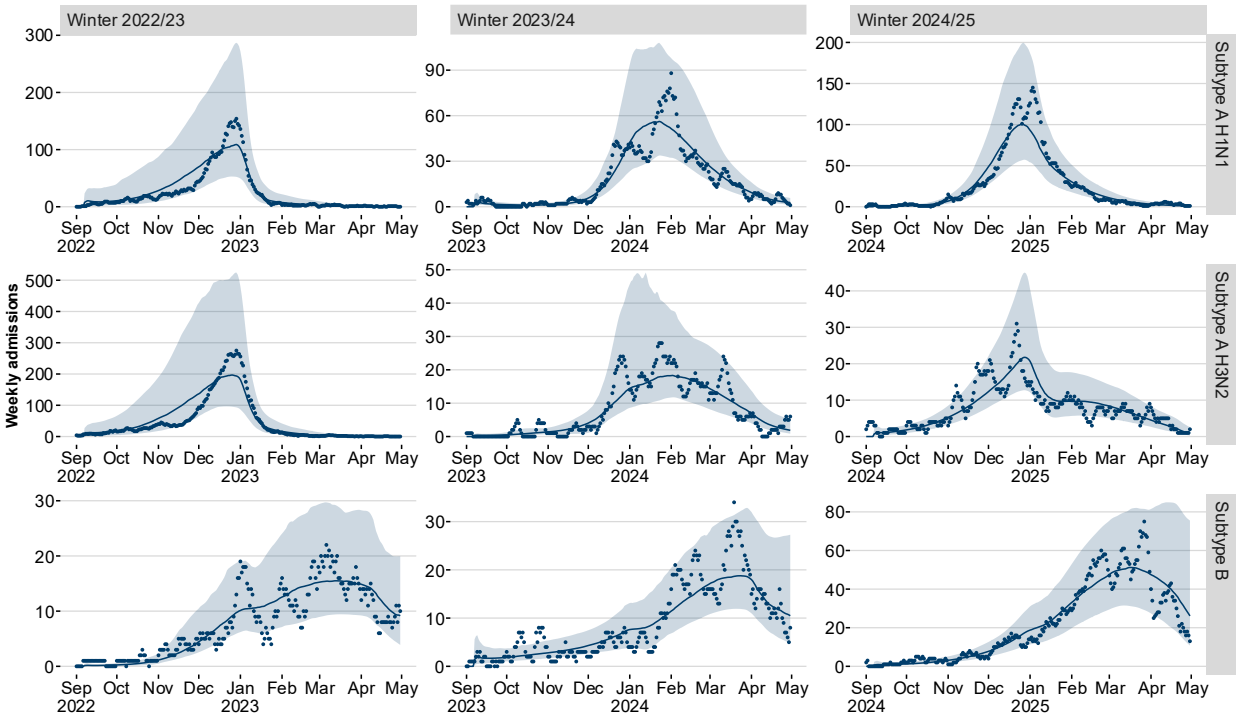

Source: SRE modelling

Note: The solid line represents the median model prediction, the dots indicate observed weekly admissions, and the shaded area shows the 95% prediction interval.

The compartment model was fitted to weekly influenza admissions data by age group and subtype in Wales separately for the winter of 2022/23, 2023/24 and 2024/25 using MCMC methods (For more details, refer to the Annex). Overall, the model showed a good fit across all influenza seasons and all three subtypes (**Figure 2-5, Table 2**). Model performance, however, varied by subtype and season.

Model performance was weakest for influenza A(H1N1) and A(H3N2) during the 2022/23 winter season **(Figure 2)**. These fits had higher weighted interval scores and consistently underestimated peak weekly admissions (**Table 2).** For example, observed A(H3N2) admissions peaked at 275 per week, whereas the model estimated a median

peak of 233 admissions, equivalent to an underestimation of approximately 15% (**Table 3**). Peak height was underestimated across all fits, most notably among adults aged 65 years and over (**Figures 6–8**). However, the calibrated model generally captured peak timing well, with the exception of the A(H1N1) fit for 2024/25, which estimated peaks earlier than observed (**Figure 4**).

Most fits showed a small, albeit positive bias with the exception of subtype B in the 2022/23 and 2024/25 winter, which showed a bias of -0.05 and -0.01 respectively (**Table 2**). The 90% interval coverage varied, ranging from 64% to 84% across different subtypes and seasons (**Table 2**).

Table 2: Performance metrics of the influenza compartment model by subtype and winter season

Season	Subtype	Weighted Interval Score	90% Interval Coverage	Bias
Winter 2022/23	Subtype A H1N1	3.84	0.84	0.23
Winter 2022/23	Subtype A H3N2	8.07	0.78	0.26
Winter 2022/23	Subtype B	1.07	0.68	-0.05
Winter 2023/24	Subtype A H1N1	2.30	0.71	0.04
Winter 2023/24	Subtype A H3N2	1.31	0.64	0.18
Winter 2023/24	Subtype B	1.30	0.71	0.11
Winter 2024/25	Subtype A H1N1	2.97	0.65	0.08
Winter 2024/25	Subtype A H3N2	1.16	0.82	0.06
Winter 2024/25	Subtype B	2.13	0.80	-0.01

Source: SRE modelling

Figure 3: Comparison of model-estimated and observed peak height in weekly influenza hospital admissions, by influenza subtype and winter season [Note 1]

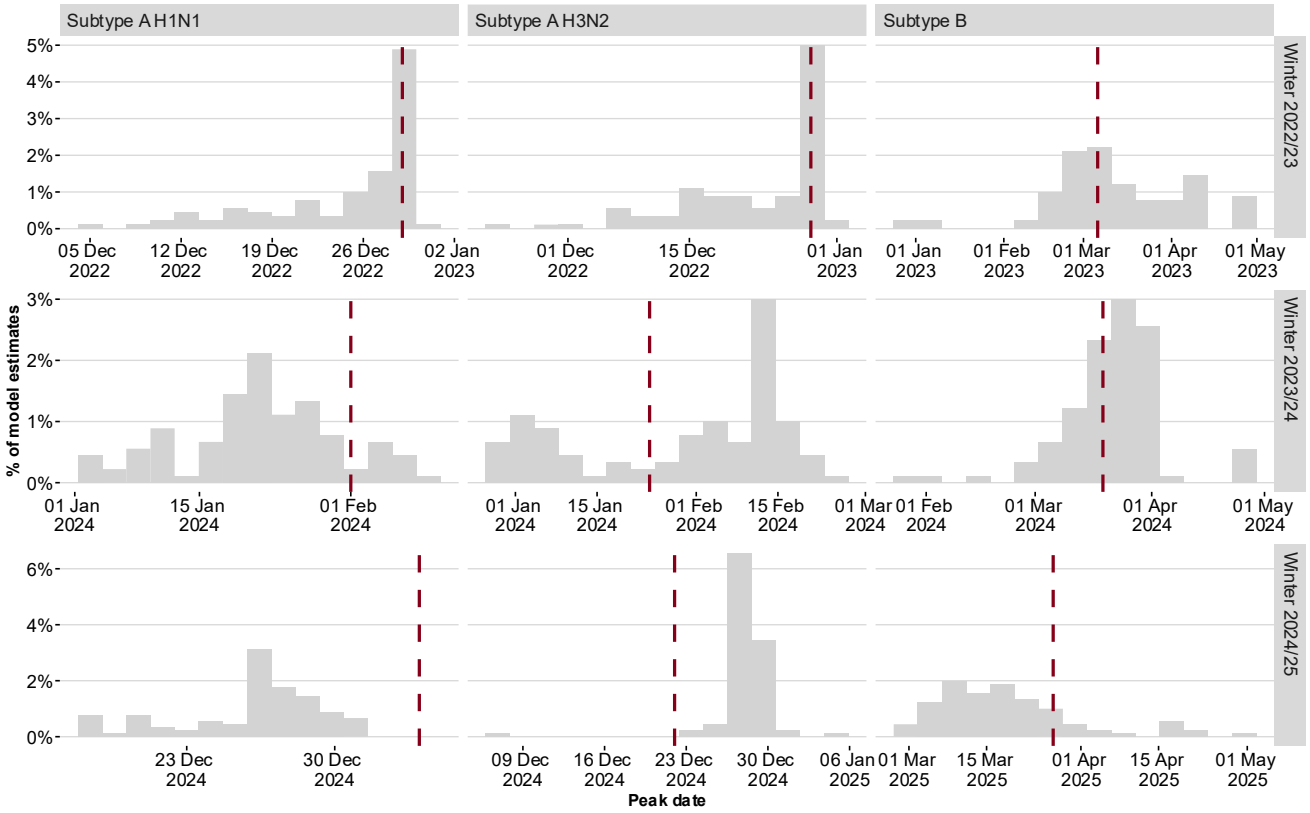

Source: SRE modelling

[Note 1]: The grey histogram shows the % of model estimates while the red vertical line shows the observed value.

Table 3: Comparison of peak estimated by model and observed data

Season	Subtype	Peak (Observed data)	Peak estimated by model	Reduction in peak height
Winter 2022/23	Subtype A H1N1	154	123.84	19.58
Winter 2022/23	Subtype A H3N2	275	232.53	15.44
Winter 2022/23	Subtype B	22	17.22	21.75
Winter 2023/24	Subtype A H1N1	88	59.34	32.57
Winter 2023/24	Subtype A H3N2	28	21.20	24.30

Winter 2023/24	Subtype B	34	20.07	40.98
Winter 2024/25	Subtype A H1N1	145	104.03	28.26
Winter 2024/25	Subtype A H3N2	31	22.50	27.43
Winter 2024/25	Subtype B	75	53.76	28.32

Figure 4: Comparison of model-estimated and observed peak date in weekly influenza hospital admissions, by influenza subtype and winter season [Note 1]

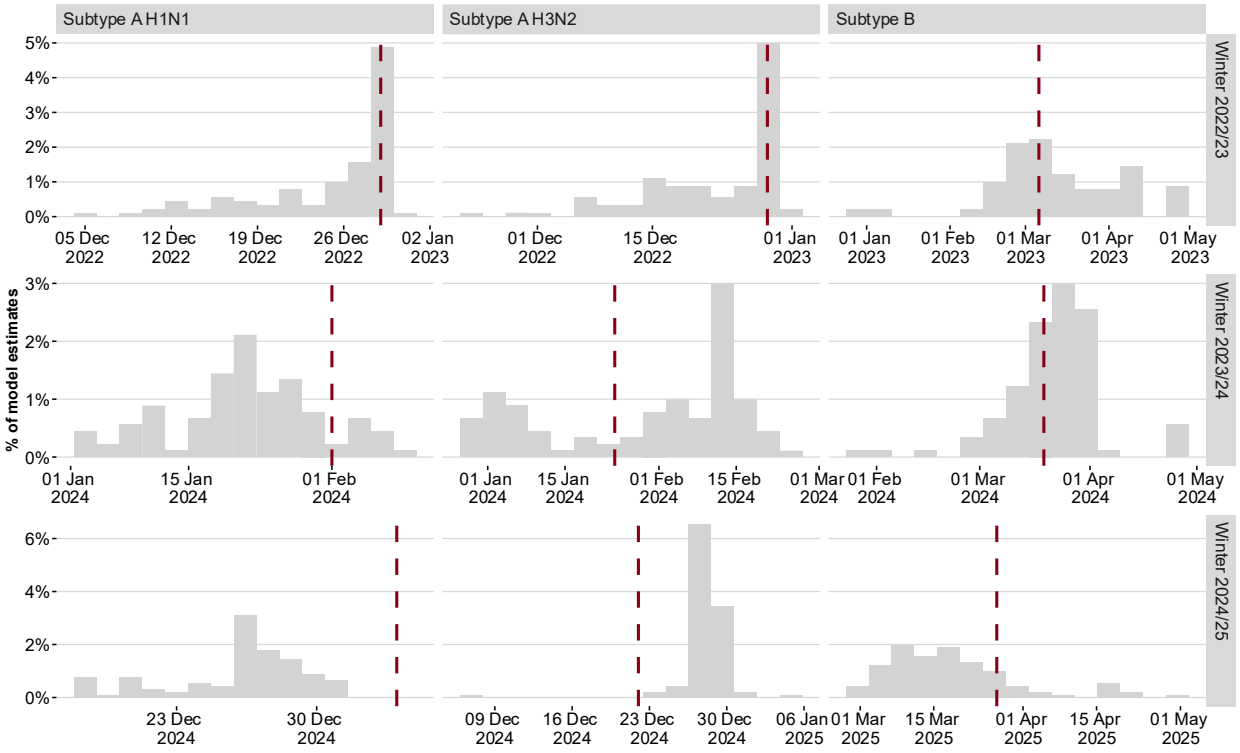

Source: SRE modelling

[Note 1]: The grey histogram shows the % of model estimates while the red vertical line shows the observed value.

Figure 5: Comparison of model-estimated and observed total number of influenza hospital admissions, by influenza subtype and winter season [Note 1]

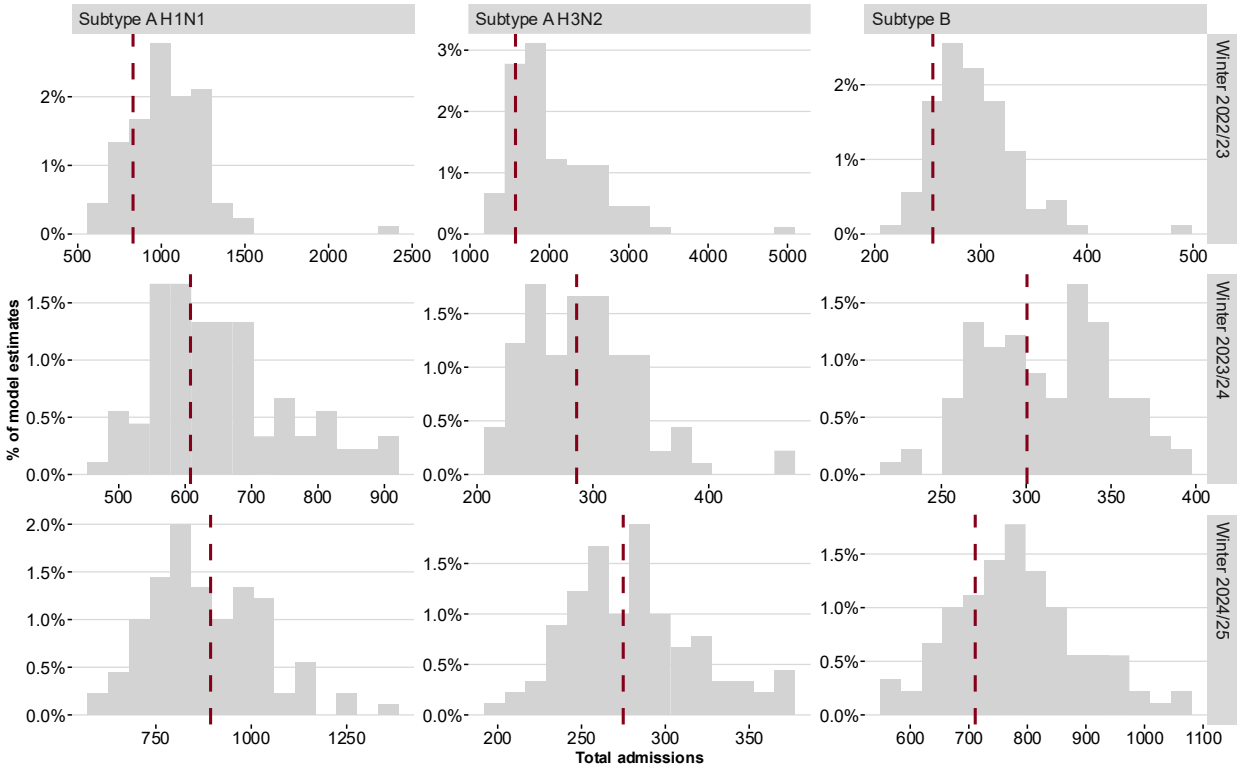

Source: SRE modelling

[Note 1]: The grey histogram shows the % of model estimates while the red vertical line shows the observed value.

Figure 6: Comparison of model fit and observed influenza admissions during the Winter 2022/23, in Wales, by age group and subtype

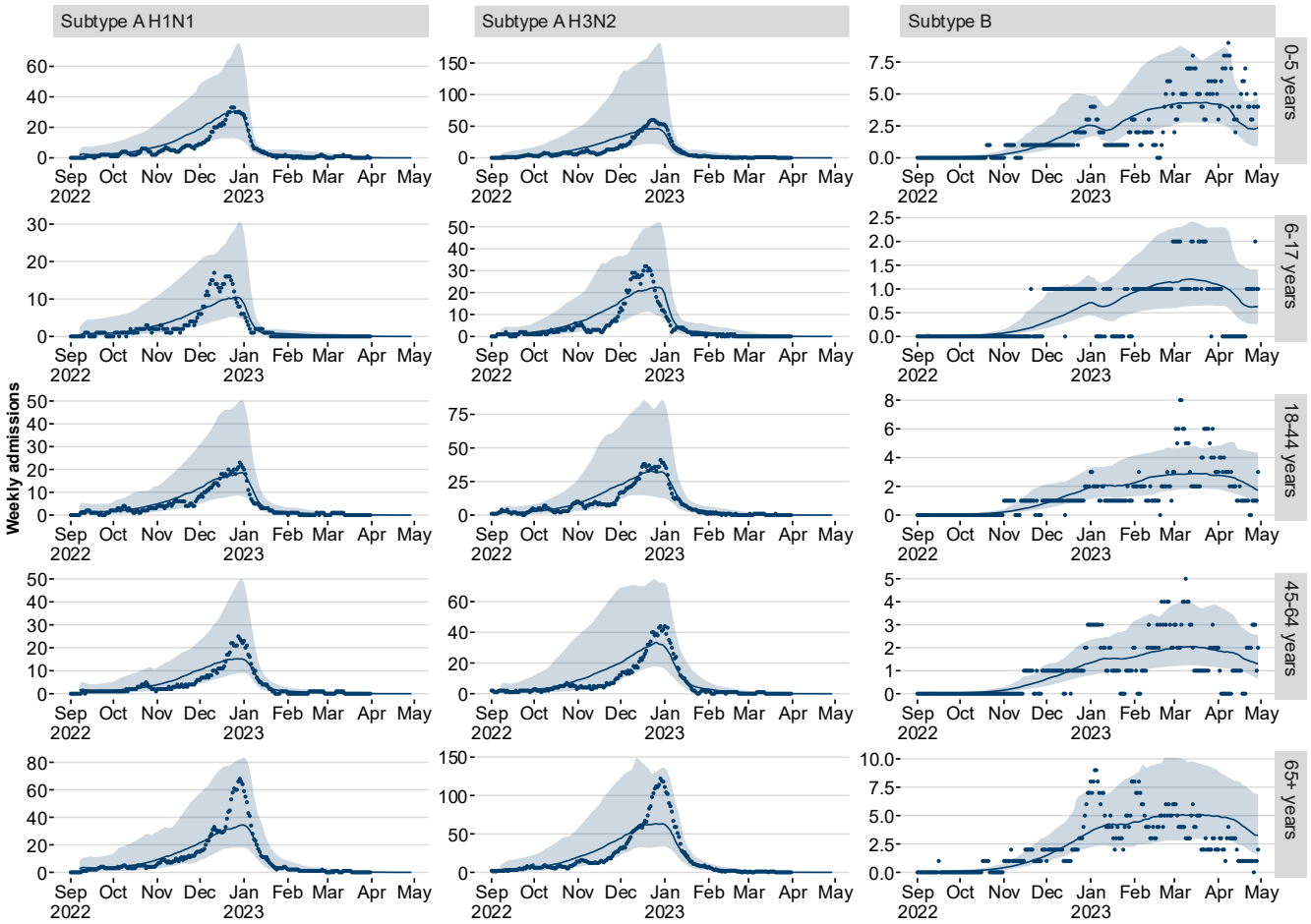

Source: SRE modelling

Figure 7: Comparison of model fit and observed influenza admissions during the Winter 2023/24, in Wales, by age group and subtype

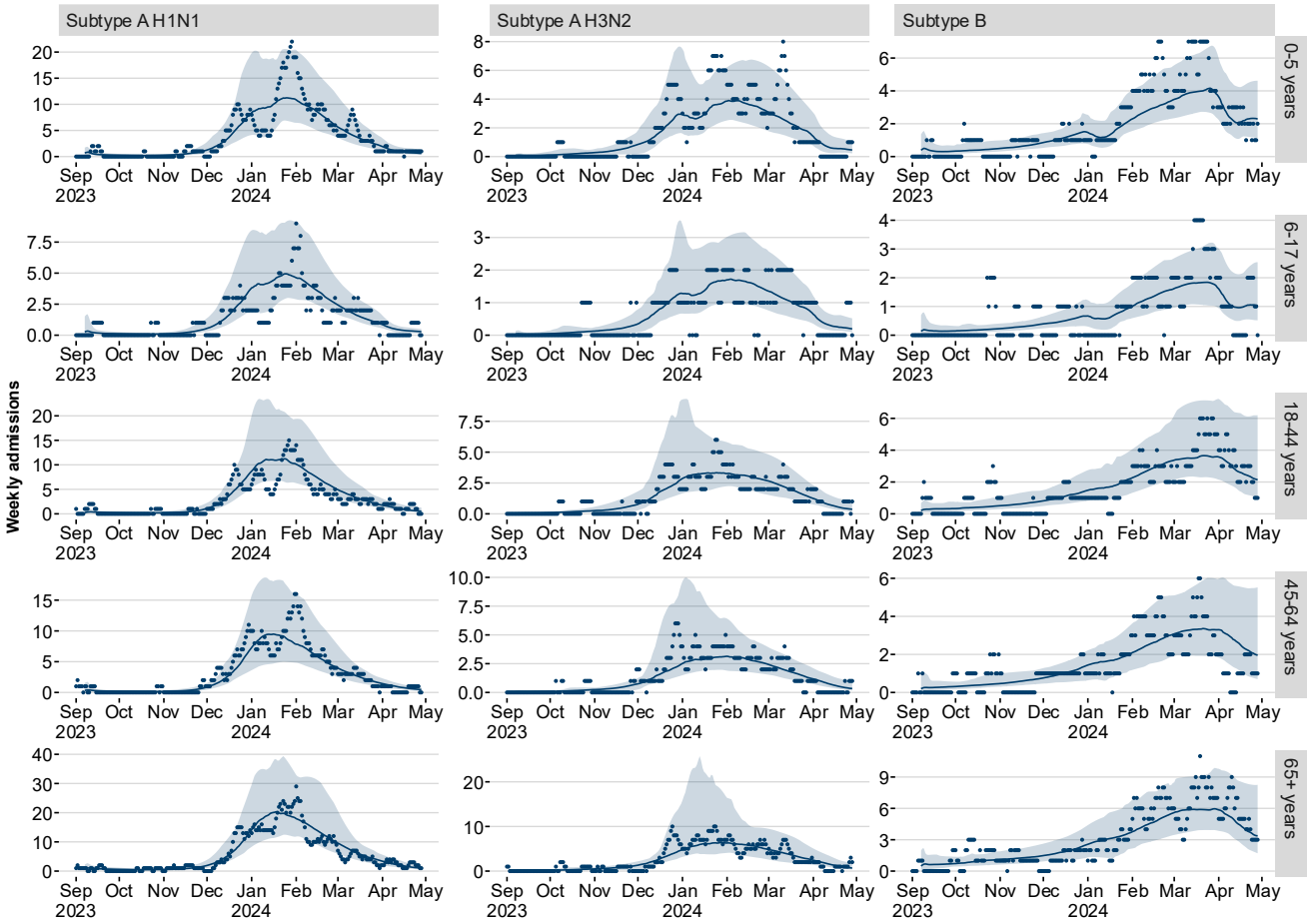

Source: SRE modelling

Figure 8: Comparison of model fit and observed influenza admissions during the Winter 2024/25, in Wales, by age group and subtype

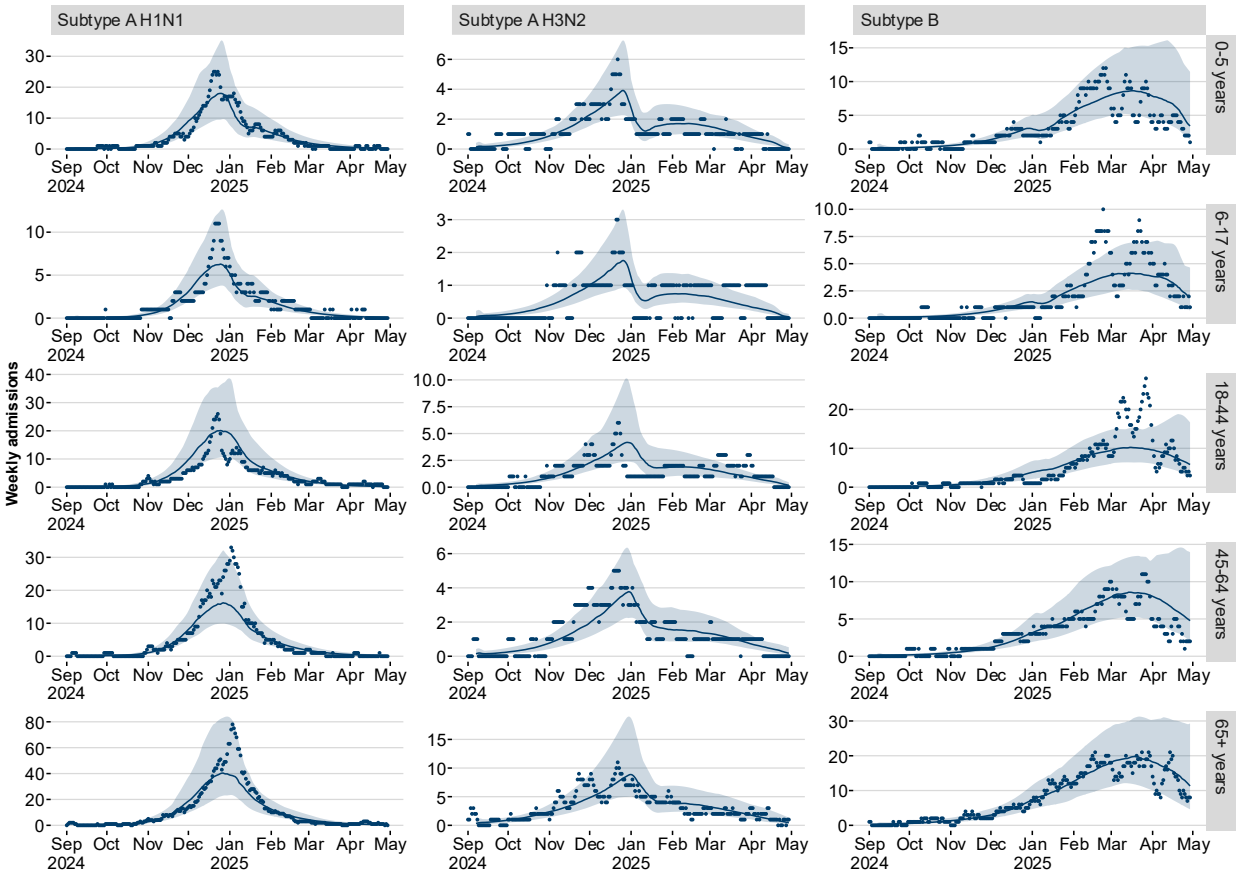

Source: SRE modelling

Posterior distributions

Using the MCMC based inference method, several key parameters were estimated that are often challenging to measure directly in epidemiological studies. Among these, R0 was evaluated by influenza subtype, and season (**Figure 9**). Median R0 ranged between 1.27 and 1.9 across all subtypes (**Figure 9**). The inferred vaccine effectiveness against infection was **generally** higher in younger age groups than in older adults. For individuals aged 0–17 years, the estimated effectiveness against infection ranged from approximately 0.22-0.46, while for those aged 65 and above, it ranged between 0.14-0.35. Additionally, estimates for the latency period and infectious period were obtained and found to be consistent with established findings in prior literature.

Figure 9: Inferred basic reproduction number (R_0), by subtype and season [Note 1]

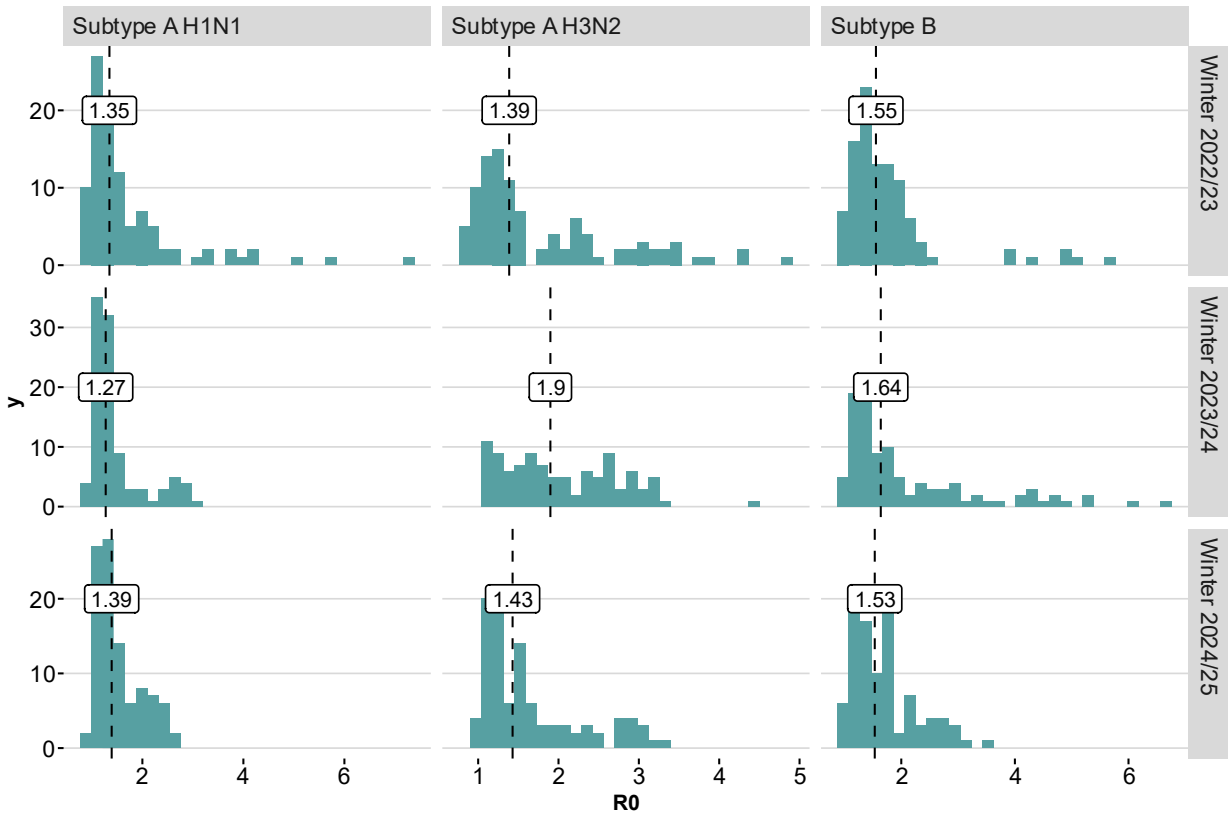

Source: SRE modelling

[Note]: Dashed line shows the median R0.

Projections and Scenario creation

The projection stage involved taking the results (i.e. posterior samples) from the fitting stage and creating a range of scenarios by varying vaccine uptake values. Vaccine effectiveness against infection was assumed to be constant. Note that, in this section, results are presented using daily hospital admissions rather than weekly admissions.

Figure 10: Influenza admissions scenarios, by subtype and season

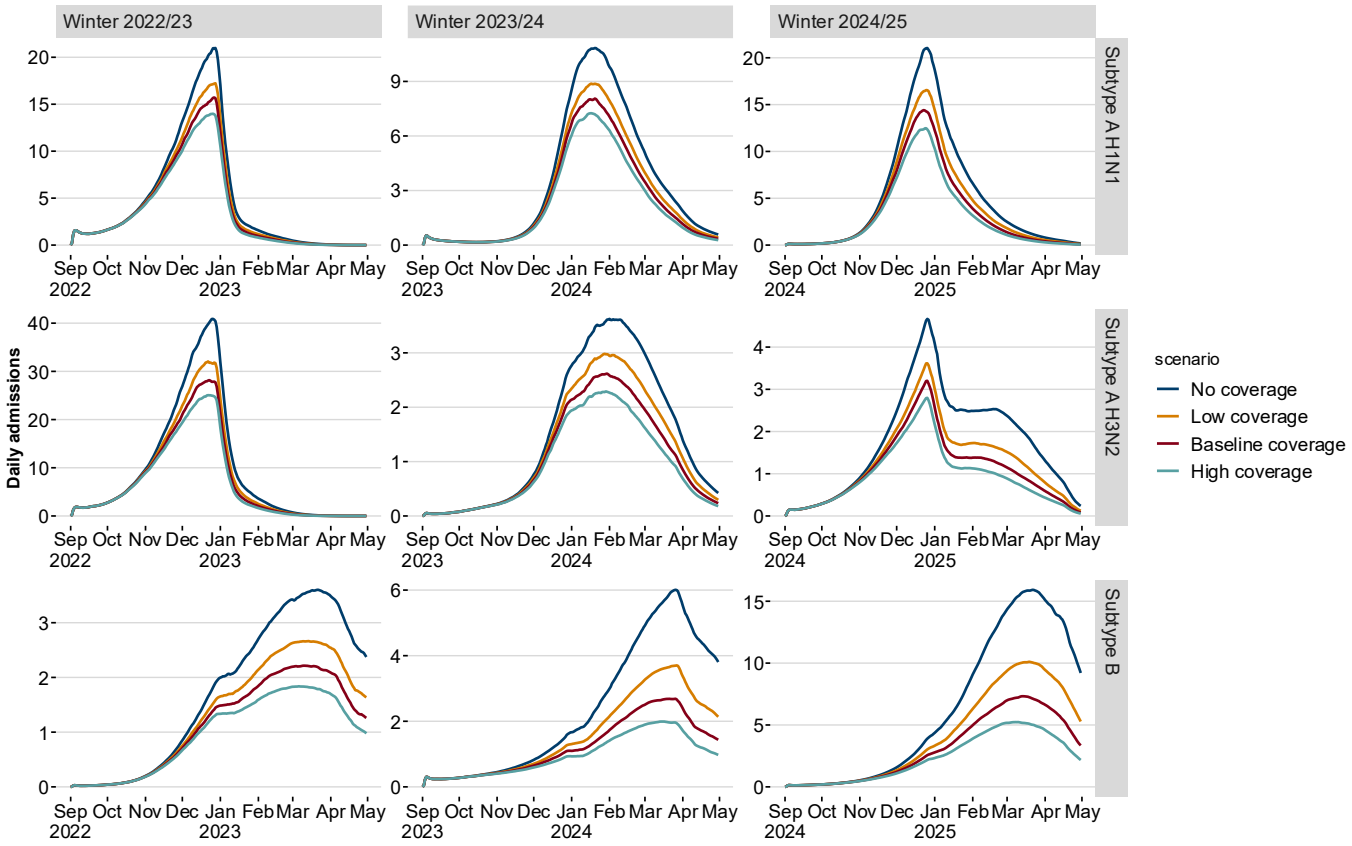

Source: SRE modelling

The no coverage scenario assumes that the vaccination programme did not take place. The baseline coverage scenario assumes vaccine uptake as observed in the respective season. The low and high coverage scenarios assume vaccination uptake that is 20% lower and 20% higher than observed, respectively. **Figure 11** shows results for the % of hospital admissions averted under different scenarios, compared to when the vaccination programme was removed.

Figure 11: Percentage of Influenza admissions averted as estimates by different scenarios, by subtype and season

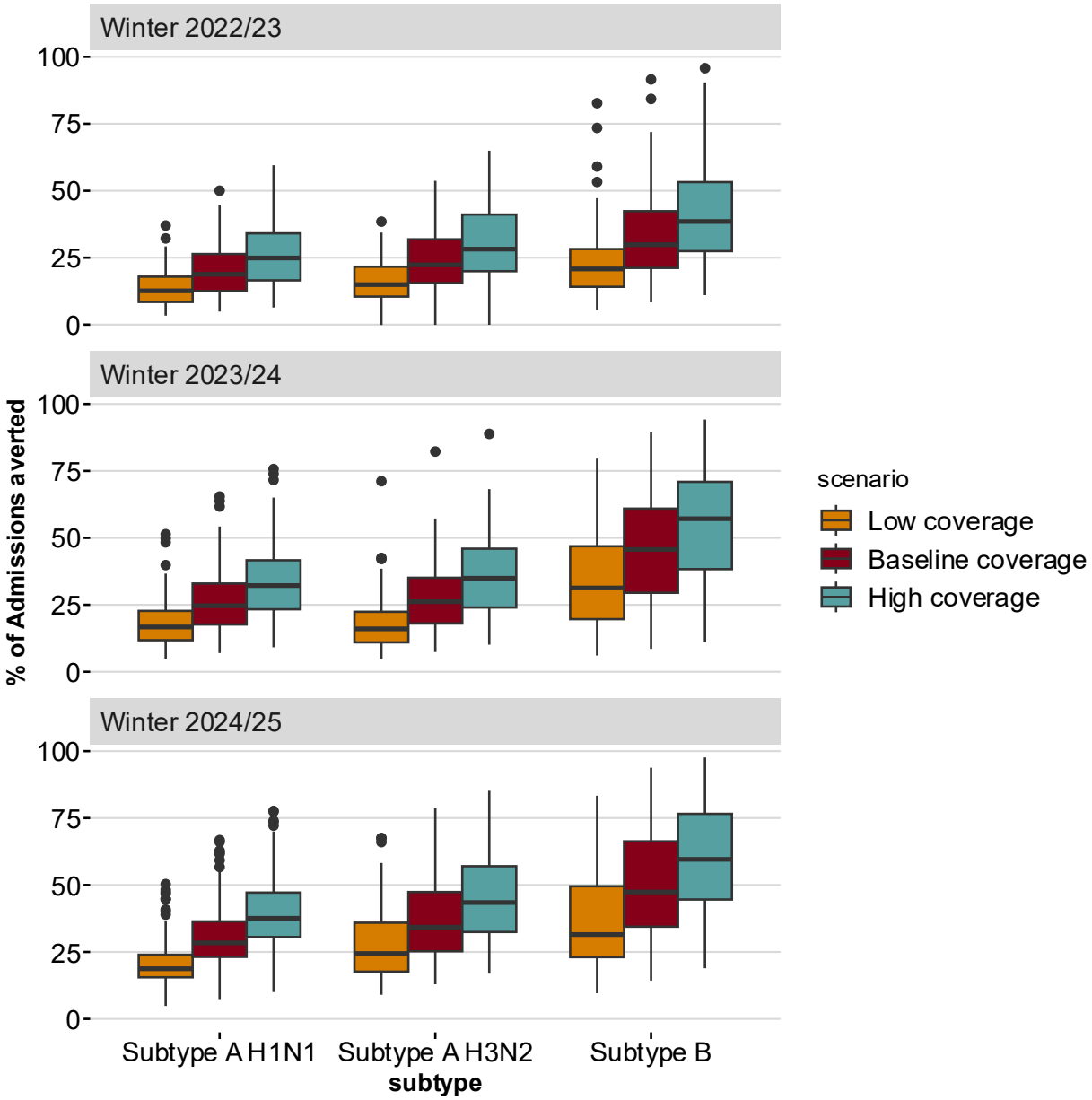

Source: SRE modelling

In the winter of 2022/23, the model estimates that 18.77% of H1N1 admissions and 22.33% of H3N2 were averted due to the vaccination programme. In comparison, a higher proportion of admissions were averted in 2023/24 and 2024/25, with 24.66 % and 28.38% of H1N1 admissions and 26.17% and 34.25% of H3N2 admissions prevented. The model also suggests that a substantial number of subtype B admissions

were averted in both seasons (29.84% in 2022/23, 45.67 % in 2023/24, 47.39% in 2024/25). Overall, while the vaccination programme resulted in a notable reduction in the total number of admissions and peak height, its impact on peak timing, was minimal.

Scenarios for 2026-27 winter modelling report

Modelling scenarios for the upcoming winter were developed by aggregating admissions across all influenza subtypes **(Figure 12).** Occupancy projections were generated using age-specific length of stay due to influenza (**Figure 13**). It is important to note that these scenarios represent potential trajectories of influenza admissions based on historic seasonal data and should not be interpreted as predictions.

Figure 12: Influenza admissions scenarios for winter 2026-27

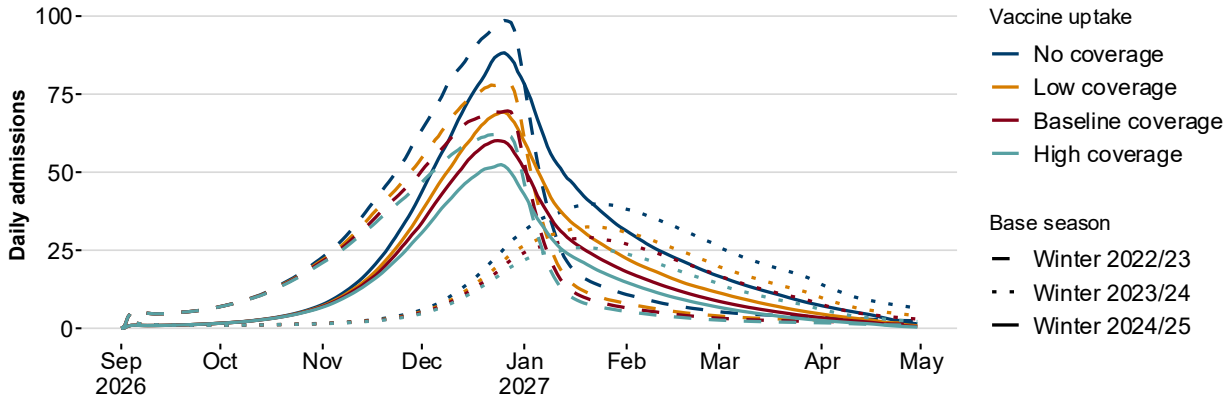

Source: SRE modelling

Admission scenarios developed using winter 2022/23 as the base season indicate that peak hospital admissions are expected to range between 62 and 99 during the last week of December (**Table 4**). In contrast, when the 2023/24 season is used as the base season, projections suggest a lower peak, with daily hospital admissions estimated to be between 26 and 40 at the highest point **(Table 4)**. Occupancy scenarios developed using winter 2022/23 project a peak of 509-865 beds used during the last week of December while 2023/24 based occupancy scenarios estimate a peak of 220-381 beds used in the last of January **(Table 5)**.

Table 4: Range of admission peak height and dates estimated by the model

Base season	Peak dates	Peak height
Winter 2022/23	24 Dec 2022 - 27 Dec 2022	62.2 - 98.6
Winter 2023/24	19 Jan 2024 - 23 Jan 2024	25.8 - 39.9
Winter 2024/25	24 Dec 2024 - 26 Dec 2024	52.4 - 88.3

Figure 13: Influenza occupancy scenarios for winter 2026-27

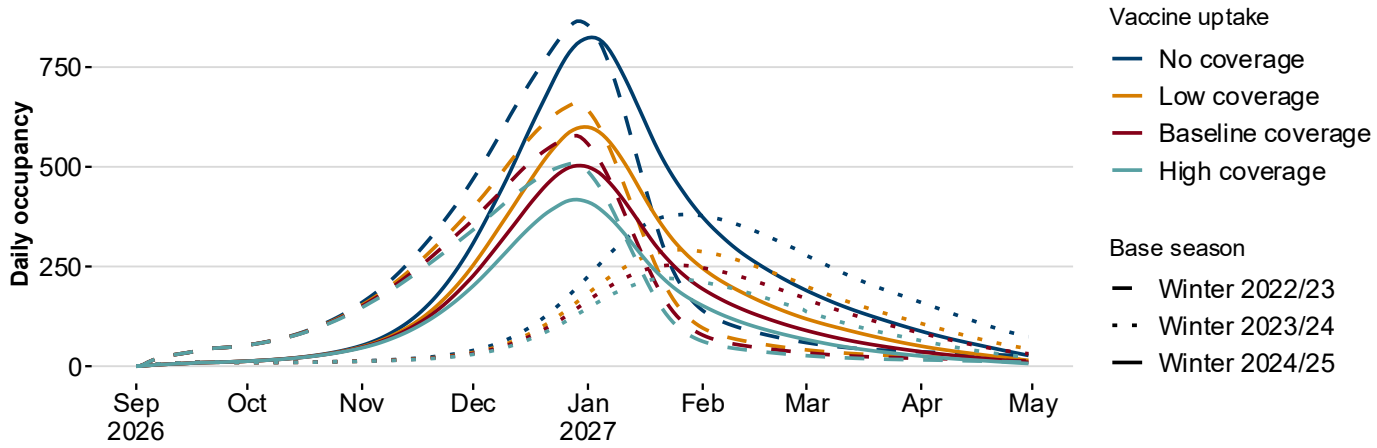

Source: SRE modelling

Table 5: Range of occupancy peak height and dates estimated by the model

Base season	Peak dates	Peak height
Winter 2022/23	28 Dec 2022 - 29 Dec 2022	509 - 865.2
Winter 2023/24	22 Jan 2024 - 27 Jan 2024	220.2 - 380.5
Winter 2024/25	29 Dec 2024 - 02 Jan 2025	417.8 - 824.6

Discussion

This paper presents an age-stratified deterministic compartmental transmission model developed to estimate and project influenza hospital admissions in Wales. The model was calibrated to observed admissions from the 2022/23, 2023/24, and 2024/25 winter seasons for influenza A(H1N1), A(H3N2), and B, and was subsequently used to construct counterfactual vaccine uptake scenarios and winter 2026/27 planning scenarios. A key strength of this approach is its dynamic transmission framework, which explicitly incorporates non-random mixing among age groups, time-varying vaccine uptake among adults aged 65 years and over and at-risk individuals aged 6–64 years, reduced transmission during school holiday periods as well as subtype-specific model calibration. Overall, the calibration results indicate that the model reproduced the broad timing and peak patterns of seasonal influenza admissions across the fitted seasons.

Our model estimates median R_0 values ranging from 1.27 to 1.9 across all influenza subtypes. These estimates are broadly consistent with the existing literature. For example, Truscott et al., using UK data, reported peak seasonal values in the range 1.6–3.[14] A systematic review by Biggerstaff et al. found a median R0 of 1.28 (IQR: 1.19–1.37) for seasonal influenza.[15] In addition, estimates of the effective reproduction number (Re) derived from epidemic growth rates are typically slightly lower: Thompson et al. reported a median Re of 1.23 for both influenza A and B, with values generally ranging from 1.10 to 1.60.[16] Overall, our modelled R0 values fall within, or slightly above, the upper end of published seasonal influenza estimates increasing the confidence in our models.

[14] **Essential epidemiological mechanisms underpinning the transmission dynamics of seasonal influenza - PMC**

[15] **Estimates of the reproduction number for seasonal, pandemic, and zoonotic influenza: a systematic review of the literature - PMC**

[16] **Global variation in early epidemic growth rates and reproduction number of seasonal influenza - ScienceDirect**

For winter planning, the modelled 2026/27 scenarios provide a range of plausible influenza admission and occupancy trajectories. Scenarios based on the 2022/23 season produced substantially higher admission and bed occupancy peaks than those based on the 2023/24 or 2024/25 season. In operational terms, the scenarios provide useful bounds for assessing potential pressure on secondary care and can support preparedness planning alongside.

The model has several limitations which should be considered when interpreting these results and the scenarios. The model excludes some vaccination groups, including healthcare workers and children under 15 years, does not represent waning natural or vaccine-induced immunity, and applies vaccine effectiveness estimates derived from England, which may not fully reflect the Welsh population. In addition, the model does not include spatial variation across local authorities and may not capture local outbreaks. Some subtype-specific fits underestimated observed peak admissions, so peak-height estimates should be interpreted with caution. Despite these limitations, the model provides a useful framework for exploring influenza transmission, vaccination impact, and potential hospital burden in Wales, with the 2026/27 outputs best interpreted as plausible planning scenarios rather than deterministic predictions.

Annex

Key assumptions

1. **Disease progression:** Infected individuals pass through a latent (exposed) period during which they are infected but not infectious, before becoming infectious. Following the infectious period, individuals recover and are removed from further transmission. There are two compartments for exposed and infectious stages to get a gamma distributed average time rather than an exponentially distributed average waiting time within these stages.

2. **Vaccination:** Vaccinated individuals are either: effectively vaccinated and moved to R_{ev}, or ineffectively vaccinated (and moved to S_v-R_v), following the same disease pathway as vaccinated individuals. The rate of transition to vaccinated compartments is dependent on time dependent vaccine uptake rate and vaccine effectiveness. Vaccination groups included in the model are adults aged 65 years and above and individuals aged 6-64 years at risk.

3. **No waning immunity:** Immunity acquired through natural infection or vaccination does not wane over the modelled period.

4. **Closed population (fixed population size):** The total population size is fixed over the modelled period. There are no births, deaths, aging or migration.

5. **Age stratification with non-random mixing:** The population is stratified by age. Contacts between age groups are governed by fixed, age-specific contact rates derived from the Reconnect survey, rather than assuming random mixing. These contact rates are not further stratified by time or setting.

6. **Reduction in attack rate during school holidays:** The force of infection is scaled down during the school holidays periods (where the contact rates in school going children are reduced by a scalar).

Data quality issues

Hospitalisation data: Admissions due to influenza were identified using ICD-10 codes J09–J11, which do not include pneumonia cases. This definition may underestimate the true number of influenza-related hospital admissions. In particular, reliance on these codes captures only cases where influenza was tested for and recorded, potentially excluding patients who were not tested or whose diagnoses have not yet been coded in clinical records.

Holidays data: The analysis assumes holiday periods based on state school calendars. This may not accurately reflect holiday timings for private schools, which can differ, and may therefore introduce some misclassification in patterns related to school holidays.

Influenza subtype data: Only a small subset of admissions are subtyped, meaning the available subtype data may not be representative of all influenza cases. In addition, subtype data are not available by age group, limiting more detailed analysis.

Vaccine uptake data: Not all general practices submit influenza uptake data on a daily basis. As a result, the dataset may be incomplete on certain days.

Reconnect survey: The survey included contacts which were face-to-face conversations or physical touch and may not account for all close encounters, such as those in crowded transport or elevators. Self-reported contacts could be affected by recall bias, and brief interactions with strangers may have been overlooked.

Differential equations

Differential equations for the compartmental model are as follows:

$$
\begin{aligned}
\frac{dS_{n,i}}{dt} &= -\lambda_i(t)S_{n,i} - \mu S_{n,i} \\
\frac{dE1_{n,i}}{dt} &= \lambda_i(t)S_{n,i} - 2\epsilon E1_{n,i} - \mu(t)E1_{n,i} \\
\frac{dE2_{n,i}}{dt} &= 2\epsilon E1_{n,i} - 2\epsilon E2_{n,i} - \mu(t)E2_{n,i} \\
\frac{dI1_{n,i}}{dt} &= 2\epsilon E2_{n,i} - 2\gamma I1_{n,i} - \mu(t)I1_{n,i} \\
\frac{dI2_{n,i}}{dt} &= 2\gamma I1_{n,i} - 2\gamma I2_{n,i} - \mu(t)I2_{n,i} \\
\frac{dR_{n,i}}{dt} &= 2\gamma I2_{n,i} - \mu(t)R_{n,i} \\
\frac{dS_{v,i}}{dt} &= -\lambda_i S_{v,i} + \mu(t)(1-\alpha)S_{n,i} \\
\frac{dE1_{v,i}}{dt} &= \lambda_i S_{v,i} - 2\epsilon E1_{v,i} + \mu(t)E1_{n,i} \\
\frac{dE2_{v,i}}{dt} &= 2\epsilon E1_{v,i} - 2\epsilon E2_{v,i} + \mu(t)E2_{n,i} \\
\frac{dI1_{v,i}}{dt} &= 2\epsilon E2_{v,i} - 2\gamma I1_{v,i} + \mu(t)I1_{n,i} \\
\frac{dI2_{v,i}}{dt} &= 2\gamma I1_{v,i} - 2\gamma I2_{v,i} + \mu(t)I2_{n,i} \\
\frac{dR_{v,i}}{dt} &= 2\gamma I2_{v,i} + \mu(t)R_{n,i} \\
\frac{dR_{ev,i}}{dt} &= \mu(t)\alpha S_{n,i}
\end{aligned}
$$

The equations below describe the counters used in hospitalizations calculations

$$
\begin{aligned}
\frac{dH_{1,i}}{dt} &= 2\gamma\eta\left(I1_{n,i} + I1_{v,i}\big(1-\alpha(H)\big)/(1-\alpha)\right) \\
\frac{dH_{2,i}}{dt} &= 2\kappa\big(H_{1,i} - H_{2,i}\big) \\
\frac{dH_i}{dt} &= 2\kappa H_{2,i}
\end{aligned}
$$

Model parameters

Table S1: Fixed parameters and priors used in the model

Parameter	Description	Value/Prior	Reference
$1/\varepsilon$	Incubation period (influenza A)	$Gamma(shape = 0.99, scale = 1.46)$days	Saito et al. 2021 [17]
$1/\varepsilon$	Incubation period (influenza B)	$Gamma(shape = 2.02, scale = 0.82)$days	Saito et al. 2021
$1/\gamma$	Infectious period (influenza A)	$Gamma(shape = 2.97, scale = 0.59)$days	Saito et al. 2021
$1/\gamma$	Infectious period (influenza B)	$Gamma(shape = 3.05, scale = 0.86)$days	Saito et al. 2021
α	Vaccine effectiveness against infection	$1 - LogNormal(-0.61, 0.29)$	van Leeuwen et al. 2025 [18]
b_0	Baseline transmissibility	$U(0,1)$	-
b_1	Seasonal forcing factor	$U(0,1)$	-
ϕ	Peak timing	$U(0,180)$days	-
ϕ	Width of the epidemic	$U(0,180)$days	-
η	Infection to hospitalization ratio	$U(0,0.5)$	-
$1/\kappa$	Delay between infection and hospitalization	$U(2,3)$ days	Campbell et al. 2010[19]

[17] **Reconstructing the household transmission of influenza in the suburbs of Tokyo based on clinical cases**

[18] **Influenza hospital admissions prevented by vaccination: a transmission dynamic analysis of the 2022/2023 and 2023/2024 programmes in England**

[19] **Risk of severe outcomes among patients admitted to hospital with pandemic (H1N1) influenza**

Likelihood calculation

The compartment model to the flu admissions data and HPV using a Markov Chain Monte Carlo (MCMC) based methods with parallel tempering to generate 500 samples from the posterior distribution. Given below is the equation for the likelihood which assumes a negative binomial equation:

$$L_{Admissions} = \prod_{i} \prod_{t} N\,egBin\left(O_{i,t}, M_{i,t}, k\right)$$

$O_{i,t}$ is the total number of observed hospital admissions for age group i at time t, $M_{i,t}$ is the hospital admissions estimated by the model and k the dispersion parameter.

Data sources

Figure S1: Demographic structure used to model influenza admissions in Wales

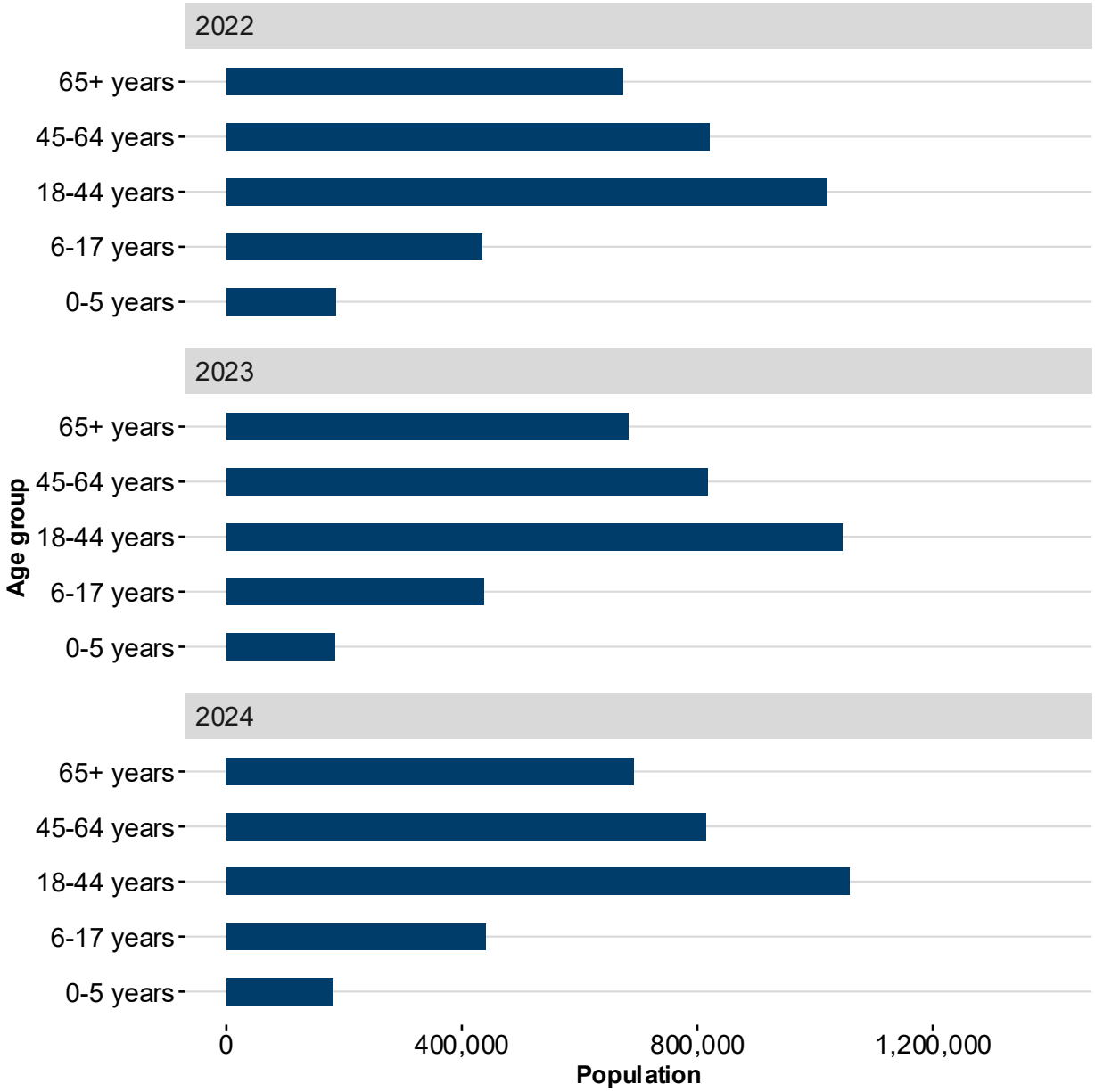

Figure S2: Contact matrix showing relative contact rates between age groups in Great Britain used in the influenza model

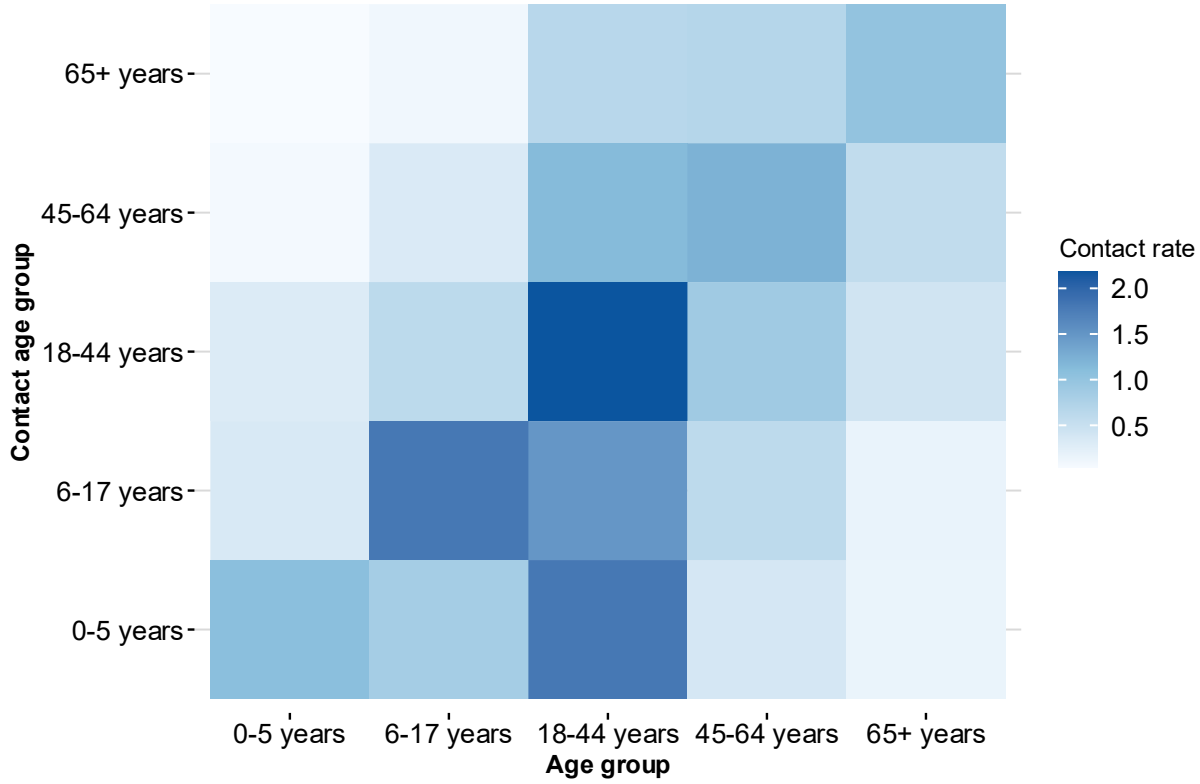

Figure S3: Length of stay due to influenza, by age group and season

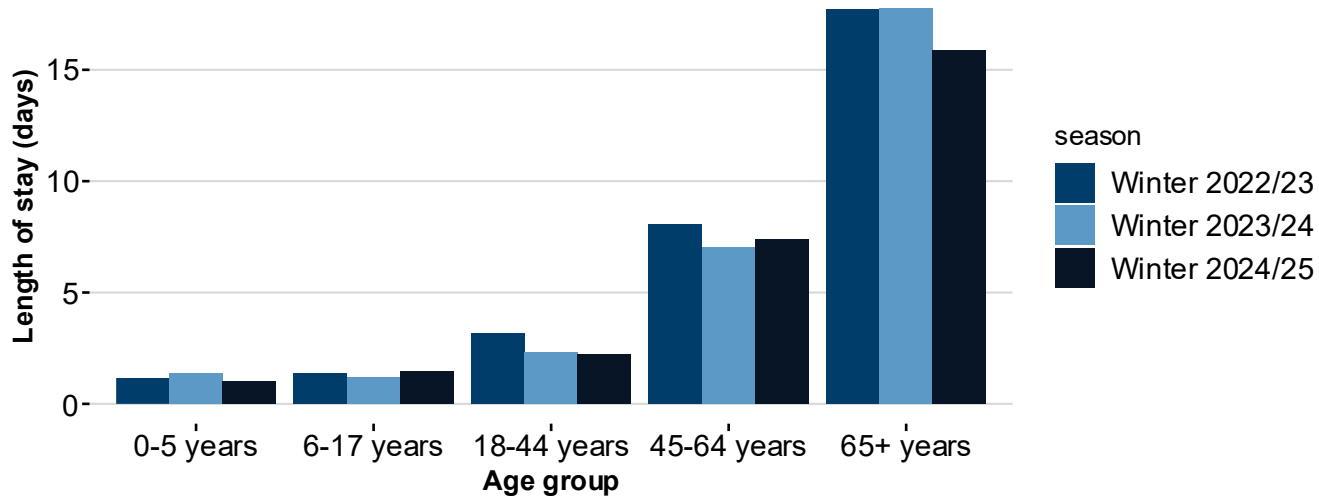

MCMC output and diagnostics

Figure S4: Trace plot of MCMC runs for Winter 2022/23

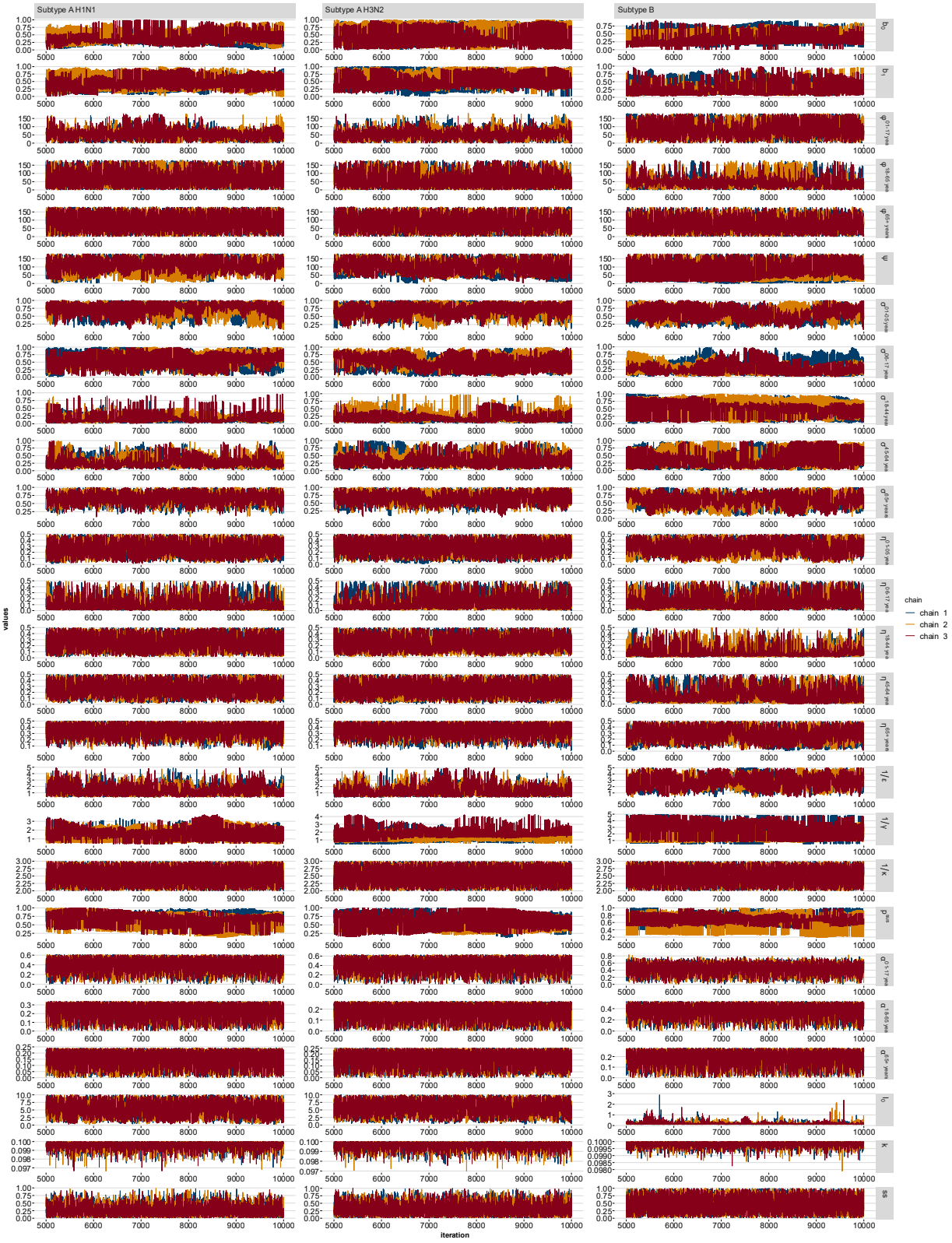

Figure S5: Trace plot of MCMC runs for Winter 2023/24

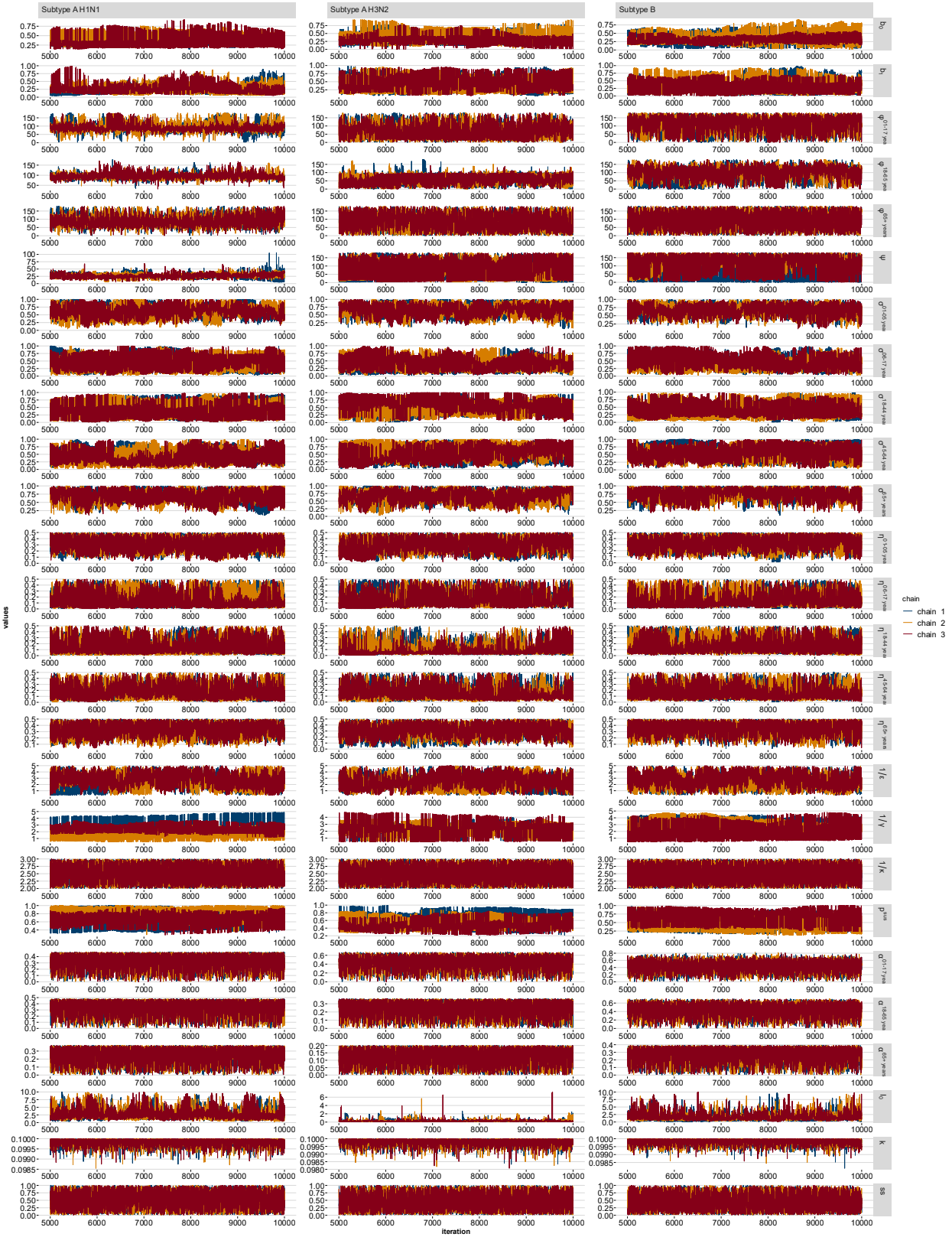

Figure S6: Trace plot of MCMC runs for Winter 2024/25

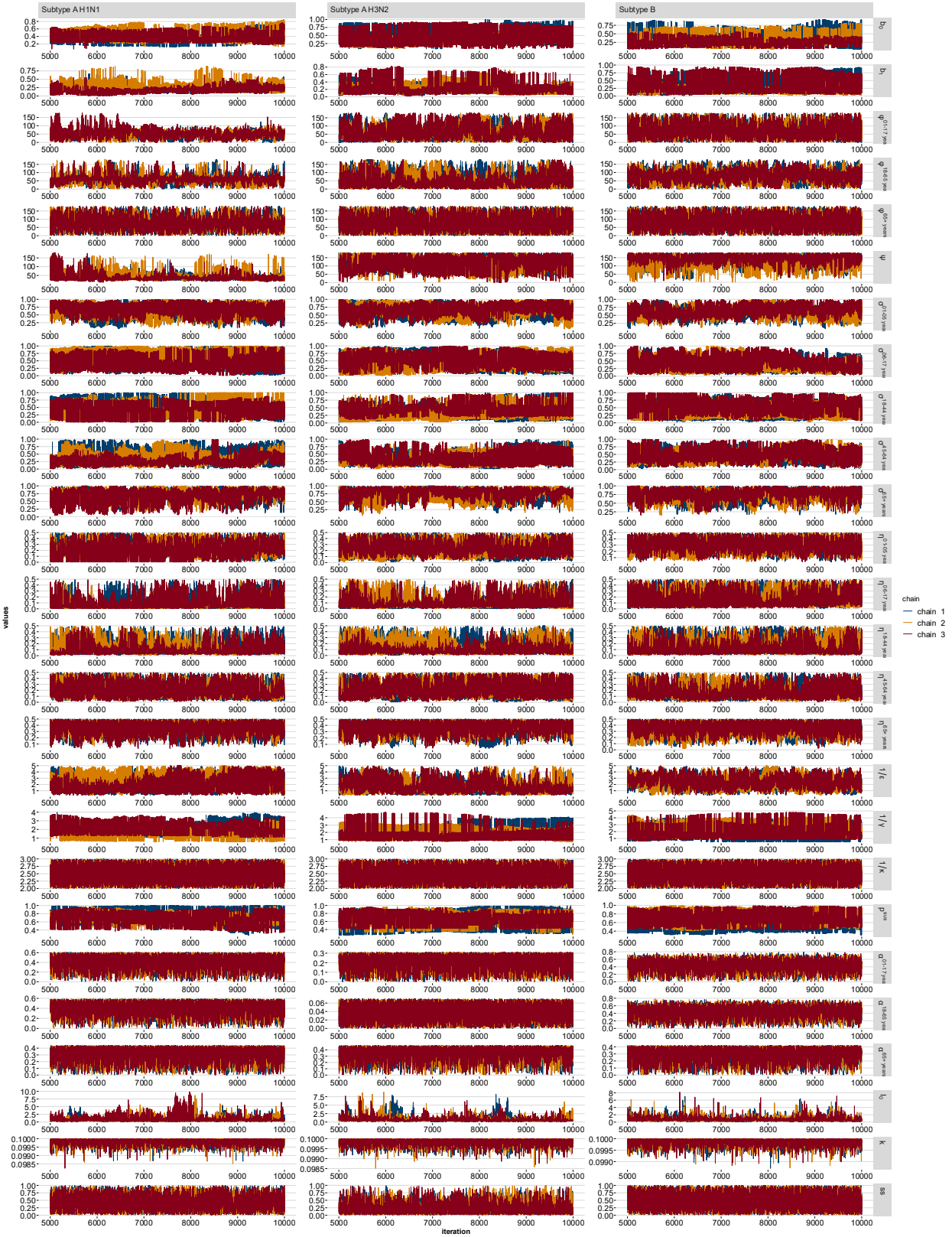

Figure S7: Posterior samples of inferred parameters for Winter 2022/23

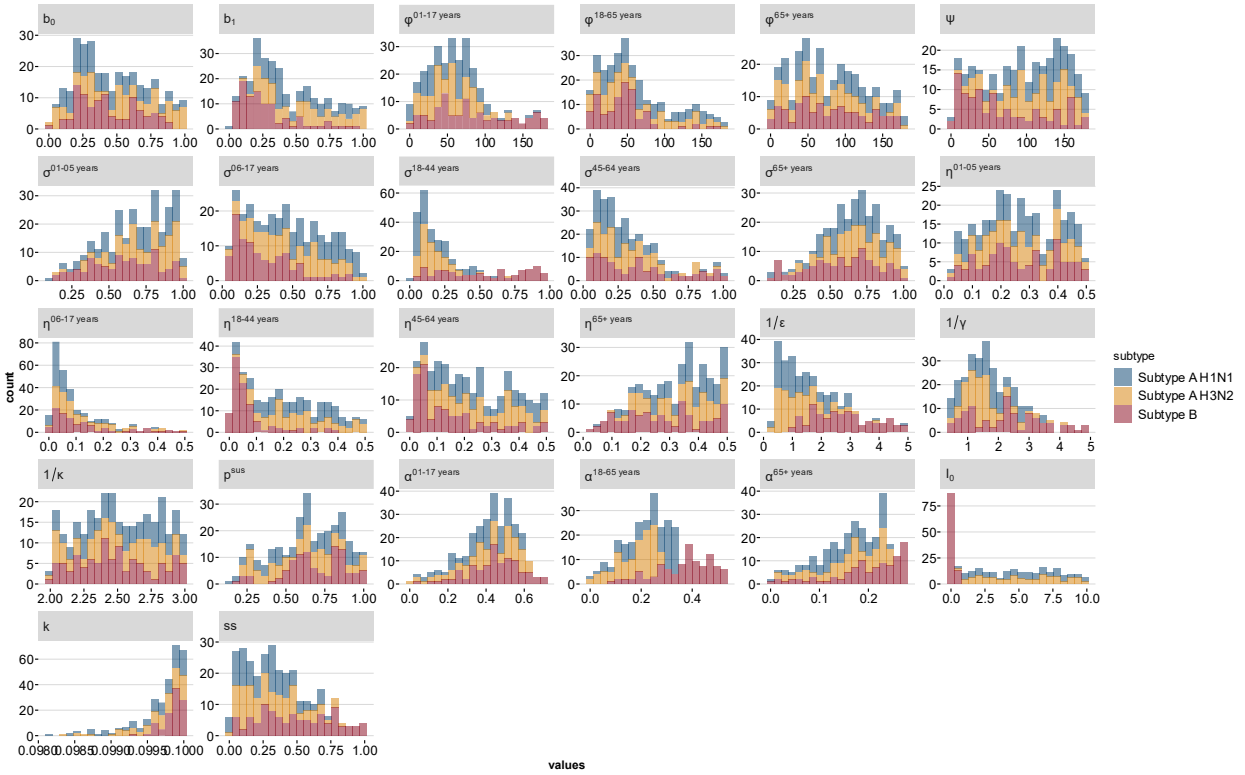

With the 9 model runs, 93.6% parameters showed Gelman-Rubin Diagnostic values <1.1. The rest (15 out of 234) showed Gelman-Rubin Diagnostic values between 1.1 and 1.25. 233 out of 234 parameters showed an effective sample size above 100.

Figure S8: Posterior samples of inferred parameters for Winter 2023/24

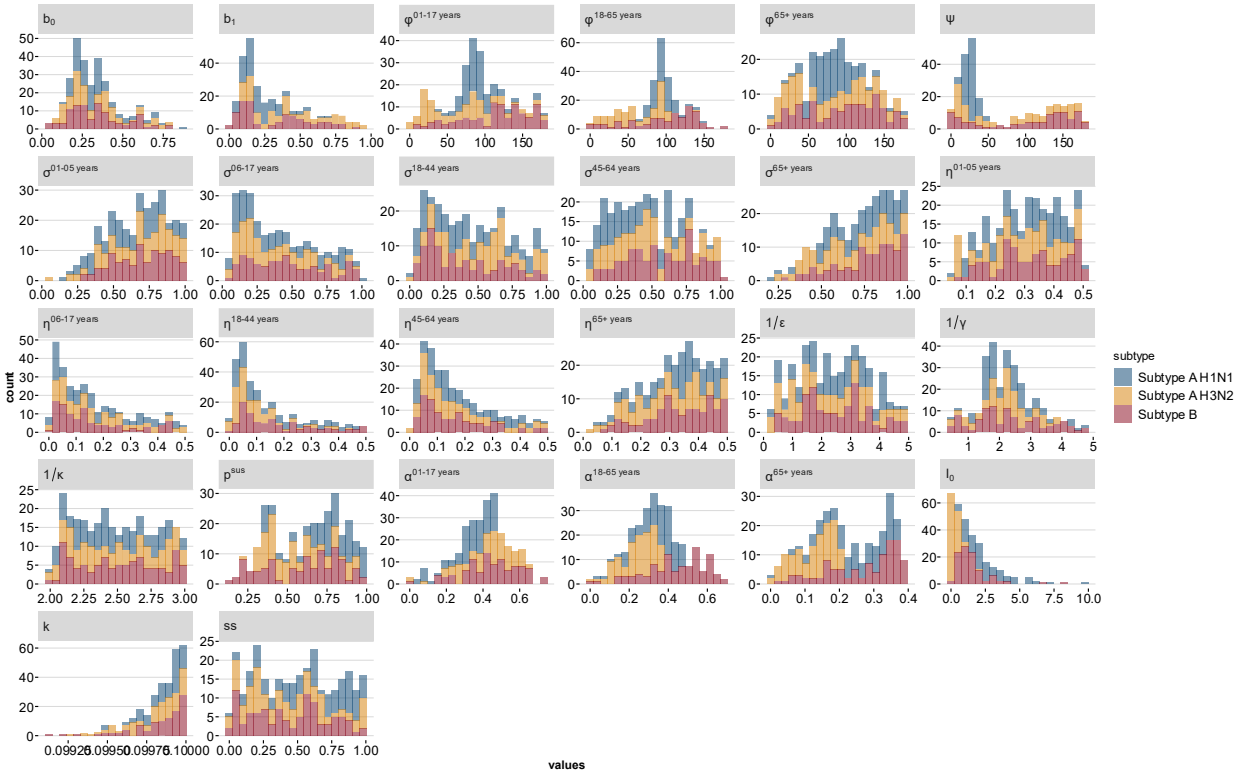

Figure S9: Posterior samples of inferred parameters for Winter 2024/25

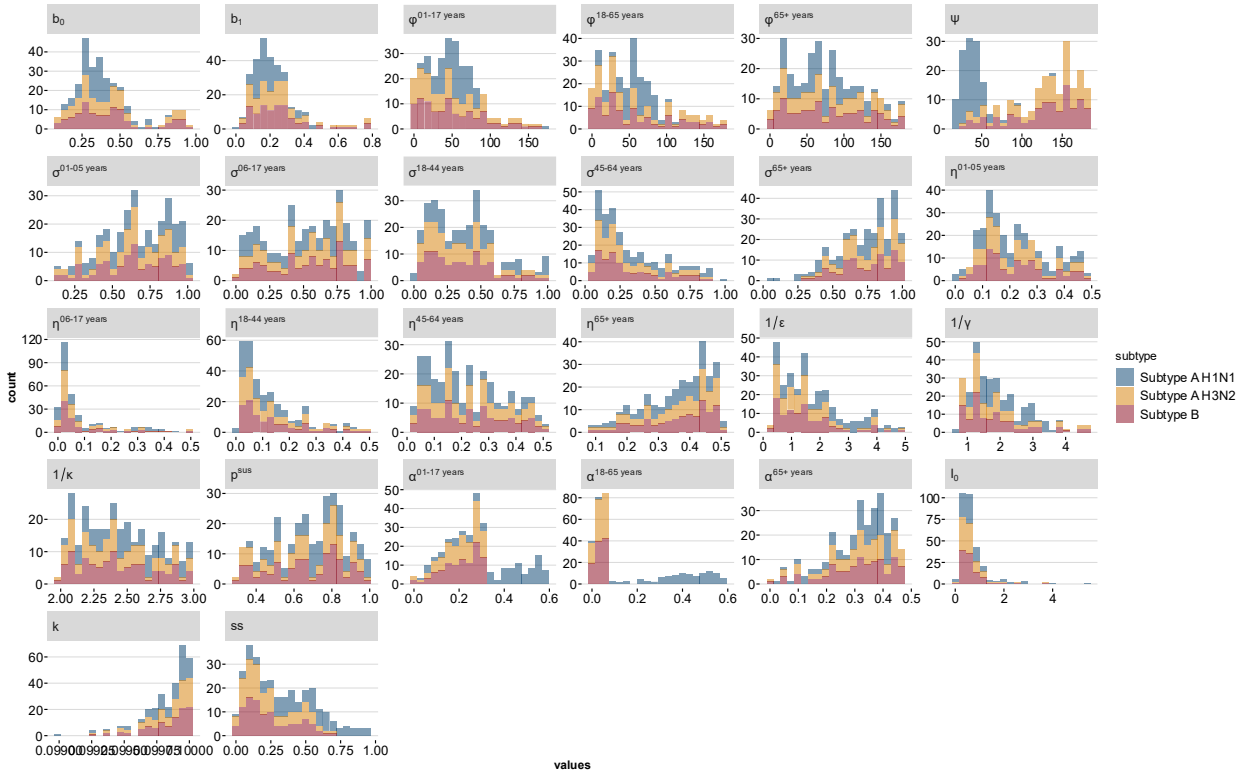

Table S2: Performance metrics of the influenza compartment model by subtype, age group and winter season

Season	Subtype	Age group	Weighted Interval Score	90% Interval Coverage	Bias
Winter 2022/23	Subtype A H1N1	0-5 years	1.39	0.67	0.49
Winter 2022/23	Subtype A H1N1	18-44 years	0.79	0.73	0.39
Winter 2022/23	Subtype A H1N1	45-64 years	0.85	0.70	0.42
Winter 2022/23	Subtype A H1N1	6-17 years	0.63	0.53	0.51
Winter 2022/23	Subtype A H1N1	65+ years	1.76	0.86	0.34

Season	Subtype	Age group	Weighted Interval Score	90% Interval Coverage	Bias
Winter 2022/23	Subtype A H3N2	0-5 years	2.73	0.75	0.42
Winter 2022/23	Subtype A H3N2	18-44 years	1.46	0.75	0.38
Winter 2022/23	Subtype A H3N2	45-64 years	1.79	0.71	0.48
Winter 2022/23	Subtype A H3N2	6-17 years	1.23	0.64	0.57
Winter 2022/23	Subtype A H3N2	65+ years	3.65	0.83	0.25
Winter 2022/23	Subtype B	0-5 years	0.55	0.44	0.29
Winter 2022/23	Subtype B	18-44 years	0.44	0.40	0.40
Winter 2022/23	Subtype B	45-64 years	0.37	0.34	0.27
Winter 2022/23	Subtype B	6-17 years	0.20	0.39	0.31
Winter 2022/23	Subtype B	65+ years	0.67	0.46	0.32
Winter 2023/24	Subtype A H1N1	0-5 years	0.72	0.56	0.12
Winter 2023/24	Subtype A H1N1	18-44 years	0.71	0.45	0.36
Winter 2023/24	Subtype A H1N1	45-64 years	0.51	0.51	0.19

Season	Subtype	Age group	Weighted Interval Score	90% Interval Coverage	Bias
Winter 2023/24	Subtype A H1N1	6-17 years	0.44	0.36	0.37
Winter 2023/24	Subtype A H1N1	65+ years	0.88	0.61	0.14
Winter 2023/24	Subtype A H3N2	0-5 years	0.44	0.40	0.26
Winter 2023/24	Subtype A H3N2	18-44 years	0.32	0.46	0.35
Winter 2023/24	Subtype A H3N2	45-64 years	0.32	0.48	0.30
Winter 2023/24	Subtype A H3N2	6-17 years	0.22	0.39	0.37
Winter 2023/24	Subtype A H3N2	65+ years	0.53	0.55	0.23
Winter 2023/24	Subtype B	0-5 years	0.46	0.50	0.05
Winter 2023/24	Subtype B	18-44 years	0.40	0.51	0.25
Winter 2023/24	Subtype B	45-64 years	0.42	0.48	0.20
Winter 2023/24	Subtype B	6-17 years	0.36	0.27	0.28
Winter 2023/24	Subtype B	65+ years	0.53	0.64	0.02
Winter 2024/25	Subtype A H1N1	0-5 years	0.65	0.52	0.34

Season	Subtype	Age group	Weighted Interval Score	90% Interval Coverage	Bias
Winter 2024/25	Subtype A H1N1	18-44 years	0.85	0.45	0.41
Winter 2024/25	Subtype A H1N1	45-64 years	0.88	0.44	0.31
Winter 2024/25	Subtype A H1N1	6-17 years	0.30	0.42	0.25
Winter 2024/25	Subtype A H1N1	65+ years	1.62	0.59	0.17
Winter 2024/25	Subtype A H3N2	0-5 years	0.28	0.53	0.19
Winter 2024/25	Subtype A H3N2	18-44 years	0.44	0.36	0.15
Winter 2024/25	Subtype A H3N2	45-64 years	0.31	0.53	0.16
Winter 2024/25	Subtype A H3N2	6-17 years	0.26	0.31	0.18
Winter 2024/25	Subtype A H3N2	65+ years	0.51	0.74	0.09
Winter 2024/25	Subtype B	0-5 years	0.66	0.56	0.26
Winter 2024/25	Subtype B	18-44 years	1.31	0.47	0.23
Winter 2024/25	Subtype B	45-64 years	0.54	0.57	0.27
Winter 2024/25	Subtype B	6-17 years	0.53	0.43	0.30

Season	Subtype	Age group	Weighted Interval Score	90% Interval Coverage	Bias
Winter 2024/25	Subtype B	65+ years	0.81	0.74	0.05